JOURNAL OF MAGNETIC RESONANCE **134,** 245–254 (1998)
ARTICLE NO. MN981541

Diffusion Measurements Using Radiofrequency Field Gradient: Artifacts, Remedies, Practical Hints

F. Humbert,[1] M. Valtier, A. Retournard, and D. Canet

Laboratoire de Méthodologie RMN,[2] Université H. Poincaré, BP 239, 54506 Vandoeuvre-lès-Nancy Cedex, France

Received February 27, 1998; revised June 12, 1998

The two major advantages of experiments carried out with radiofrequency (RF) field-gradient NMR are the instrumental simplicity and the insensitivity to background static magnetic field gradients. These features combined with large RF gradients, which became available only recently, should make this technique especially attractive for molecular translational diffusion studies. However, a critical evaluation of the method shows that under some circumstances (small and/or heterogeneous samples, weak diffusion coefficients, very short relaxation times) the quality of measurements may be affected by a number of artifacts. Their origin has been investigated and several remedies have been considered; in particular, a new improved sequence is presented. The success of various experimental tests demonstrates the efficiency of the proposed solutions which thus open the way to much wider application fields.

Key Words: **NMR; diffusion; radiofrequency field gradient.**

INTRODUCTION

It is well established that the *p*ulsed-*f*ield-*g*radient (PFG) NMR technique provides a suitable means for investigating molecular translational diffusion in a wide variety of systems. Actually, two methods exist. The oldest and the most common one uses the static magnetic field gradient and is based on the pulsed gradient spin echo (PGSE) experiment (*1, 2*). During the last decade, advances in B_0 gradient technology have led to significant improvements in terms of switching, shielding, mechanical stability, and cooling efficiency. Moreover, in order to overcome the problem of background gradients, very large applied gradients (for small samples) are now available. Another solution lies in numerous modified sequences in more or less complicated fashion (*3–6*). The second method, that we are concerned with here, uses the radiofrequency (RF) magnetic field gradient (*7, 8*). The latter has two major advantages over the former: insensitivity to susceptibility inhomogeneities (*9*) and instrumental simplicity. Actually this technique does not suffer from all the problems mentioned above about B_0 gradients, and therefore can accommodate non-sophisticated probe arrangement and simple pulse sequences. Nevertheless, the main difficulty is to produce strong uniform RF field gradients, the largest amplitude obtained to date being 75 G cm^{-1} at 90 MHz for a volume of 3 mm × 3 mm × 3 mm (*10*). Although this is almost an order of magnitude smaller than B_0 gradients, its capability to achieve similar spatial resolution has been demonstrated. For such an experimental arrangement the RF field amplitude ranges from 17 to 32 G across the sample. These values are high enough to preclude any off-resonance effect and sufficiently small so as one can disregard background gradients. A last advantage of B_1 gradient pulses stems from negligible rise and fall times (by contrast to B_0 gradients) and, all together, the technique should be ideally suited for diffusion studies in heterogeneous systems such as plant materials, porous media, and zeolites which in addition possess very short transverse relaxation times.

The basic experiment is depicted in Fig. 1. In the case of unrestricted diffusion, for a sample with a single resonance line, the signal amplitude S is given by (*8, 11*)

$$S(\delta, \Delta) = \frac{M_0}{2} \exp\left(\frac{-2\delta}{T_{12}}\right) \exp\left(\frac{-\Delta}{T_1}\right) \times \exp\left(-\gamma^2 g_1^2 \delta^2 D\left[\Delta + \frac{2\delta}{3}\right]\right), \quad [1]$$

where M_0 is the magnitude of the equilibrium magnetization, T_1 is the longitudinal relaxation time, T_{12} is the time constant characterizing relaxation during the RF pulses, g_1 is the RF gradient strength, δ is the length of the gradient pulses, Δ is the diffusion interval, D is the self-diffusion coefficient, and γ is the gyromagnetic ratio.

Neglecting the relaxation during RF pulses and setting $\Delta \gg 2\delta/3$, expression [1] becomes

$$S(\delta, \Delta) = \frac{M_0}{2} \exp\left(\frac{-\Delta}{T_1}\right) \exp(-\gamma^2 g_1^2 \delta^2 D \Delta). \quad [2]$$

Thus, under these conditions, the signal attenuation due to translational diffusion should be purely exponential. Nevertheless, a detailed assessment reveals that in some situations (see

[1] To whom correspondence should be addressed.
[2] UPRESA CNRS 7042, FU CNRS E008 (INCM).

1090-7807/98 $25.00

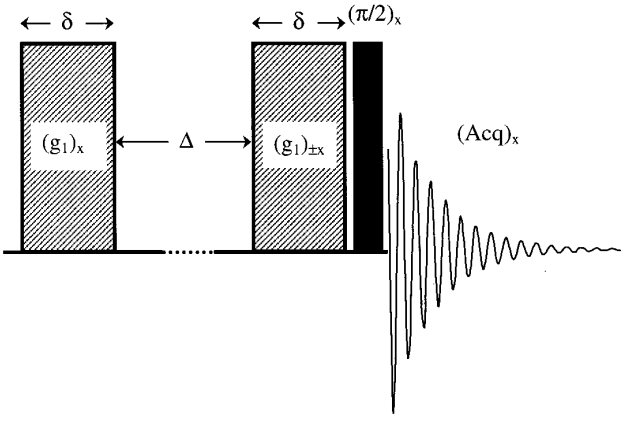

FIG. 1. The basic sequence for studying translational molecular motion with RF field gradients. The hatched rectangles represent RF gradient pulses of duration δ and magnitude g_1. The diffusion interval is denoted by Δ. The two-step phase cycle permits us to retain only the longitudinal magnetization which is measured by the homogeneous $\pi/2$ read pulse.

thereafter) the expected exponential behavior is affected by a number of artifacts. In this paper, we analyze their origin and we present an improved pulse sequence capable of circumventing these artifacts and which consequently expands the range of applications of the technique. Moreover we give some practical hints for measuring reliably small diffusion coefficients ($<10^{-6}$ cm^2 s^{-1}) and also procedures adapted to the study of systems with short relaxation times T_{12}. The measurements presented here were carried out with a Bruker Biospec BNT 100 operating at 100 MHz and with a homebuilt spectrometer equipped with a 2.1-T electromagnet. For both spectrometers the RF probe includes a flat concentric two-turn coil generating the B_1 gradient and a Helmholtz coil for collecting the NMR signal and producing homogeneous pulses (for more details see Ref. (*10*)).

ANALYSIS OF THE BASIC SEQUENCE

This section is devoted to an overview of the theoretical background leading to expression [2]. Let X be the spatial direction of the RF gradient and consider an elementary slice at a given abscissa X corresponding to an equilibrium magnetization m_0. Taking explicitly into account the two steps of the phase cycle given in Fig. 1 and normalizing to one acquisition, it is easy to demonstrate that, immediately after the $\pi/2$ read pulse, the magnetization components are

$$\begin{aligned} m_x &= m_0 E_2 \sin\theta \sin\psi \\ m_y &= \mp m_0 E_2 \sin\theta \sin\theta' \cos\psi \\ &\quad + m_0(1-E_1)\cos\theta + m_0 E_1 \cos\theta \cos\theta' \\ m_z &= m_0 E_2 \sin\theta \cos\theta' \cos\psi \\ &\quad \pm m_0(1-E_1)\sin\theta \pm m_0 E_1 \cos\theta \sin\theta', \end{aligned} \qquad [3]$$

that is, dropping terms which cancel due to the phase cycling,

$$\begin{aligned} m_x &= m_0 E_2 \sin\theta \sin\psi \\ m_y &= m_0(1-E_1)\cos\theta + m_0 E_1 \cos\theta \cos\theta' \\ m_z &= m_0 E_2 \sin\theta \cos\theta' \cos\psi, \end{aligned} \qquad [4]$$

where ψ is the precession angle during Δ; $E_1 = \exp(-\Delta/T_1)$ and $E_2 = \exp(-\Delta/T_2^*)$ (T_2^* the effective transverse relaxation time); and θ and θ' are the nutation angles due to the first and second gradient pulse, respectively.

The important point is that, although the durations of both gradient pulses are identical, θ' can be different from θ because of translational molecular motions along the X direction during Δ. This can be accounted for by expressing θ' in the form $\theta + \varphi$ where the angle φ is the nutation deviation arising exclusively from the diffusional motion (*7*). If we are concerned only with molecular self-diffusion, a molecule has an equal probability of moving in the direction of the field gradient or in the opposite direction. Consequently, considering a time average (denoted below by a bar) over the translational motions which occur during the interval Δ, $\overline{\sin\varphi} = 0$ and the m_y component can be written as

$$\overline{m_y} = m_0(1-E_1)\cos\theta + m_0 E_1 \cos^2\theta \overline{\cos\varphi}. \qquad [5]$$

At this stage, one usually considers (*8, 11*) that the gradient pulses are sufficiently long so as to induce a complete defocusing of the macroscopic magnetization, in such a way the ensemble averages (over the sample) can be written $\langle\cos\theta\rangle = 0$, $\langle\sin\theta\rangle = 0$, $\langle\sin^2\theta\rangle = \frac{1}{2}$, and $\langle\cos^2\theta\rangle = \frac{1}{2}$. Thus the whole magnetization component M_x is zero whereas M_y is given by

$$\overline{M_y} = M_0 \frac{E_1}{2} \overline{\cos\varphi} \qquad [6]$$

leading to the detected signal amplitude given in Eq. [2], since for unrestricted diffusion (*2*),

$$\overline{\cos\varphi} = \exp(-\gamma^2 g_1^2 \delta^2 D \Delta). \qquad [7]$$

However, it has been sometimes observed that the signal attenuation versus $(g_1\delta)^2$ deviates from a pure exponential exhibiting oscillations and important data scattering. These artifacts are more or less pronounced depending on the size of the object under investigation, on its structural heterogeneity, and on the values of Δ/T_1, g_1, δ, and D. In an attempt to elucidate the origin of these anomalies, it can be useful to revisit the approximation of complete magnetization defocusing and in particular to concentrate on the following points: (1) Is this approximation always experimentally justified? (2) If not, what are the consequences? (3) Is there an alternative?

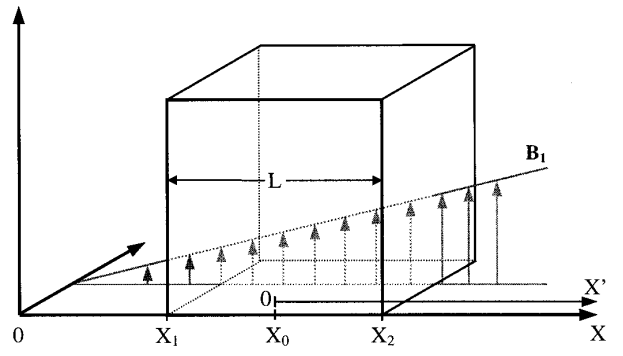

FIG. 2. Schematic diagram showing a parallelepipedic sample of length L, centered at the abscissa X_0 and subjected to a RF gradient along the direction X. The vertical arrows stand for the B_1 gradient amplitude.

To answer these questions let us first analyze the term cos θ appearing in the above relations. At abscissa X the nutation angle θ can be written as $\theta = \gamma g_1 X \delta$ or by defining a reciprocal space variable k, $\theta = 2\pi k_x X$ with $k_x = (2\pi)^{-1}\gamma g_1 \delta$. This simple relation is the basis of NMR imaging using RF field gradients (*12*). It can be recalled that, with this technique, k-sampling along the k_x axis is performed by measuring the transverse magnetization for incremented values of the gradient pulse width, δ, and that the Fourier transform of the resulting pseudo-FID yields the spin density profile along the X axis. Therefore it is obvious that $\langle \cos\theta \rangle$ can be noticeably different from zero depending on the δ and g_1 values but also on the size and heterogeneity of the object under investigation. For example, consider a homogeneous box of length L, the RF gradient being applied parallel to one side X (Fig. 2). The space average of cos θ is

$$\langle \cos\theta \rangle = \frac{1}{L}\int_{X_1}^{X_2} \cos(\gamma g_1 X \delta) dX$$

$$\langle \cos\theta \rangle = \frac{1}{L}\int_{-L/2}^{L/2} \cos(\gamma g_1 (X' + X_0)\delta) dX' \quad \text{with } X' = X - X_0$$

$$\langle \cos\theta \rangle = \cos(\gamma g_1 X_0 \delta)\mathrm{sinc}\left(\frac{\gamma g_1 L \delta}{2}\right),$$

where the sinc symbol has its usual meaning ($\mathrm{sinc}(x) = (\sin x)/x$)

$$\langle \cos\theta \rangle = \cos\theta_0 \mathrm{sinc}\left(\frac{\gamma g_1 L \delta}{2}\right) \qquad \text{with } \theta_0 = \gamma g_1 X_0 \delta. \quad [8]$$

In the same way,

$$\langle \cos^2\theta \rangle = \frac{1}{2}[1 + \cos(2\theta_0)\mathrm{sinc}(\gamma g_1 L \delta)]. \quad [9]$$

Therefore combining Eqs. [8], [9], [7], and [5], an expression for the detected signal can be written as

$$S(\delta, \Delta) = M_0\left[(1 - E_1)\cos\theta_0 \mathrm{sinc}\left(\frac{\gamma g_1 L \delta}{2}\right) + \frac{E_1}{2}\exp(-\gamma^2 g_1^2 \delta^2 D\Delta) \times [1 + \cos(2\theta_0)\mathrm{sinc}(\gamma g_1 L \delta)]\right] \quad [10]$$

or

$$S(\delta, \Delta) = M_0 \frac{E_1}{2}\exp(-\gamma^2 g_1^2 \delta^2 D\Delta)[1 + C]$$

with

$$C = \frac{2(1 - E_1)}{E_1 \exp(-\gamma^2 g_1^2 \delta^2 D\Delta)}\cos\theta_0 \mathrm{sinc}\left(\frac{\gamma g_1 L \delta}{2}\right) + \cos(2\theta_0)\mathrm{sinc}(\gamma g_1 L \delta). \quad [11]$$

This latter relation demonstrates that the signal attenuation versus $(g_1\delta)^2$ is not purely exponential and may exhibit oscillations due to the sinc function. As an illustration, let us examine two limiting cases:

(a) $\Delta \ll T_1$. In this case E_1 goes to one and Eq. [10] becomes

$$S(\delta, \Delta) \approx M_0 \frac{E_1}{2}\exp(-\gamma^2 g_1^2 \delta^2 D\Delta) \times [1 + \cos(2\theta_0)\mathrm{sinc}(\gamma g_1 L \delta)] \quad [12]$$

and, as a consequence of the sinc function, the deviation from an exponential gets significant as the $g_1\delta$ product is weak or/and L is small. This latter point can be especially crucial in the study of small or heterogeneous samples as well as for localized diffusion measurements.

(b) $\Delta > T_1$. For the study of systems with both short relaxation times T_1 and small diffusion coefficients, it is necessary to set Δ larger than T_1. Thus E_1 becomes very small and Eq. [10] may be approximated by

$$S(\delta, \Delta) \approx M_0 \cos\theta_0 \mathrm{sinc}\left(\frac{\gamma g_1 L \delta}{2}\right). \quad [13]$$

The signal is here simply modulated by a function which corresponds to the Fourier transform of the spin density profile of the box along the X direction. This effect is particularly clear in Fig. 3. Moreover Fig. 4 shows that Eq. [10] describes the experimental data quite adequately.

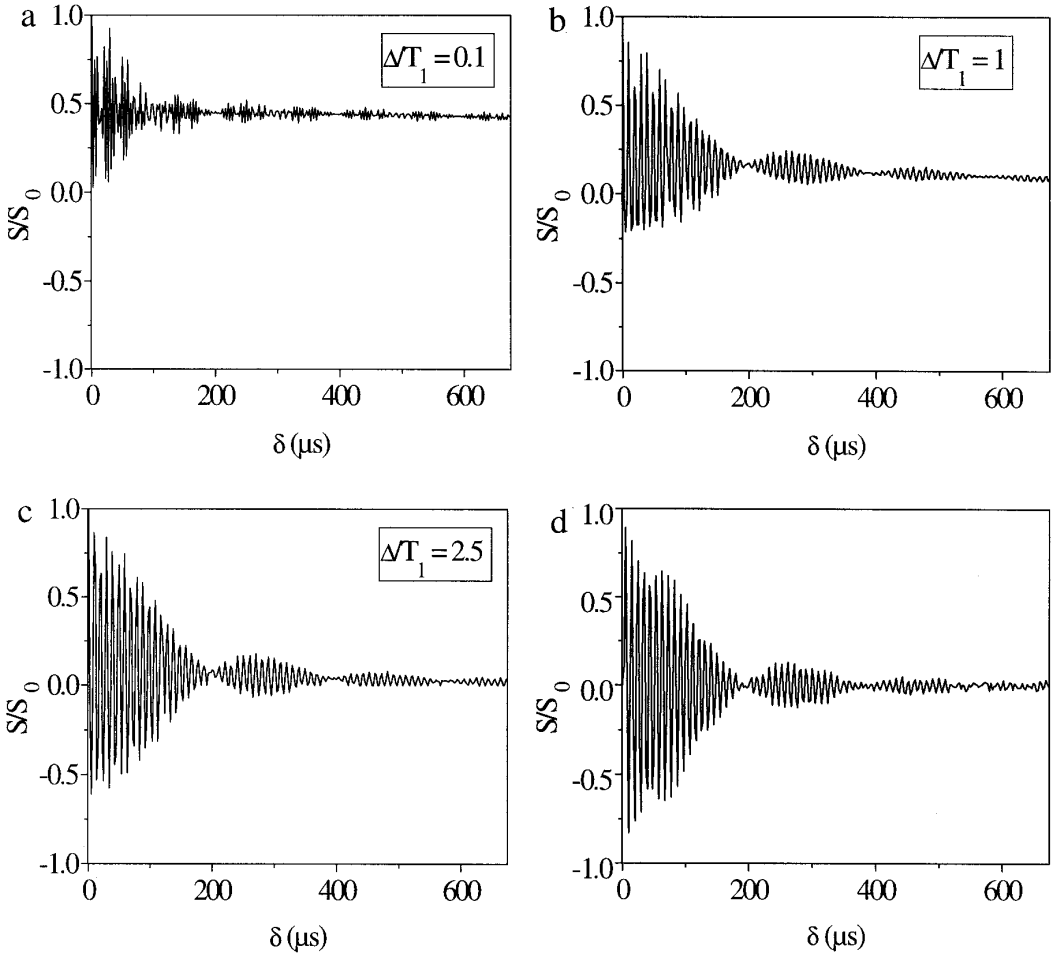

FIG. 3. Parts (a), (b), and (c) are plots of the relative signal attenuation S/S_0 versus the gradient pulse width δ, obtained by the sequence in Fig. 1 for three Δ/T_1 ratios. The sample is a teflon box ($2 \times 2 \times 0.23$ mm) filled with octanol. It was installed perpendicularly to the B_1 gradient direction so as to set the length L (Fig. 2) at 230 μm. Note that when the Δ/T_1 ratio increases, this response approaches the pseudo-FID (d) corresponding to the Fourier transform of spin density profile of the sample along the X direction. Number of transients = 256; repetition time = 2.5 s; g_1 = 52 G cm^{-1}; T_1 = 460 ms; D = 1.4 10^{-6} cm^2 s^{-1}.

Of course, in view of Eq. [11], a solution to minimize the quantity C is to increase the argument of the sinc function, that is, $\gamma g_1 L\delta$ and in particular δ, hence the usual requirement of *sufficiently long* pulses. However, due to limitations of RF power amplifiers such as the maximum pulse width (between 10 and 20 ms), the maximum duty cycle (about 10%), and the droop effects, the pulse duration cannot be increased indefinitely. Moreover, as illustrated in Fig. 5, the quantity C (Eq. [11]) does not decrease continuously when δ increases. Indeed, above a certain δ value, the first term in the right-hand side of Eq. [10] becomes the major term. Note also from Fig. 5, that in some circumstances, the quantity C remains larger than 1% and even 5% irrespective of the values of δ. In a general way, these effects become more accentuated for short L, g_1, T_1, and T_{12} values and large Δ and Δ/T_1 values.

IMPROVED PULSE SEQUENCE

Artifacts described in the previous section should disappear as long as the θ modulation is removed from Eq. [5]. Concerning the second term in the right-hand side of Eq. [5], one method for reaching this objective while retaining the $\overline{\cos\,\varphi}$ term associated with diffusion is to annihilate the squared cosine modulation by combining it with a squared sine modulation. This can be achieved by inserting appropriate homogeneous $\pi/2$ pulses in the basic sequence so as to arrive at the new experiment shown in Fig. 6. It consists of two subsequences A and B. The A subsequence differs from the basic sequence (Fig. 1) only by the initial π pulse of the second phase step which, concomitantly with the acquisition sign change, enables one to cancel the first term in the right-hand side of Eq. [5]. Indeed, immediately after the last $\pi/2$ read

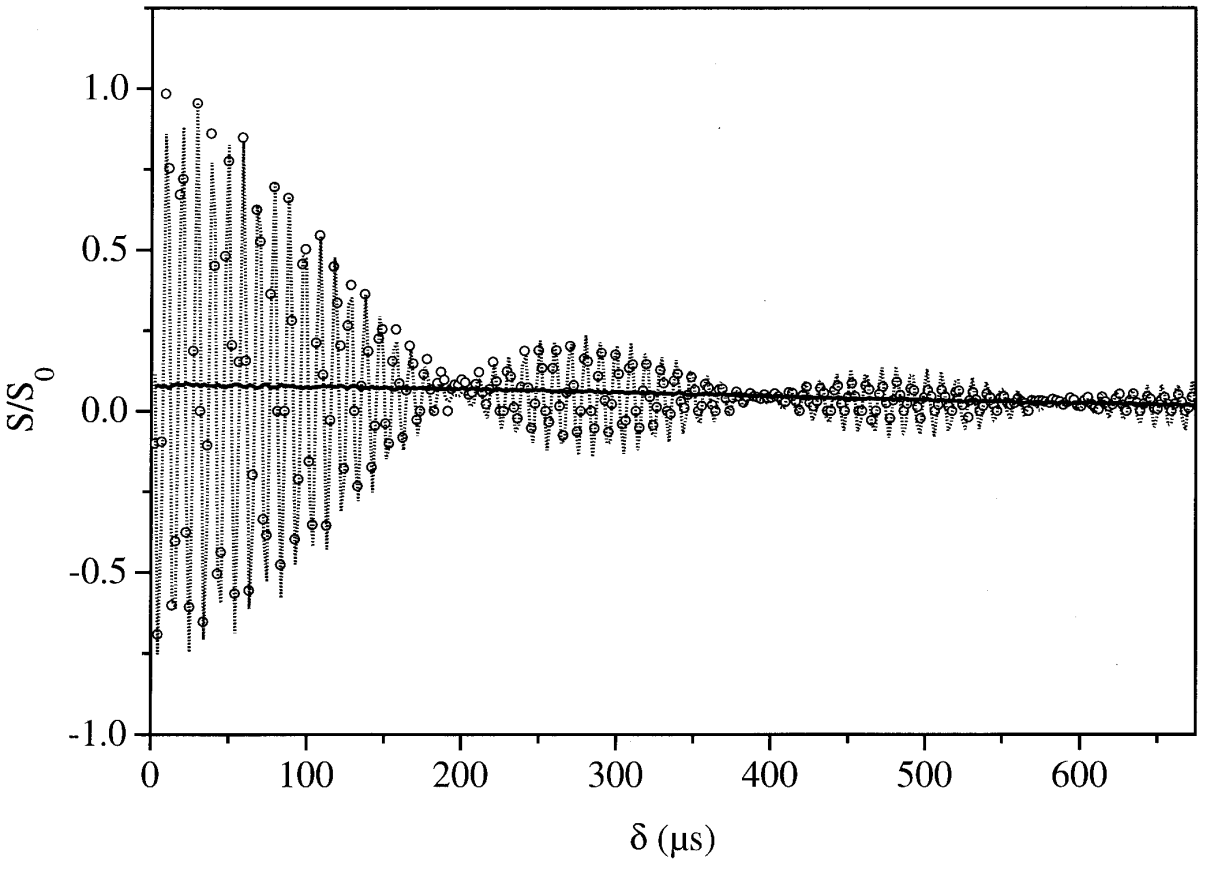

FIG. 4. Comparison of the experimental data (○) of Fig. 3c with the theoretical curve obtained from Eq. [10] and $g_1 = 52$ G cm^{-1}; $T_1 = 460$ ms; $D = 1.4\ 10^{-6}$ cm^2 s^{-1}; $L = 230$ μm; $\Delta = 1.12$ s; apparent π pulse duration (gradient coil) = 4.9 μs. The solid curve (—) corresponds to experimental data obtained by the improved pulse sequence (Fig. 6) which totally eliminates the oscillations.

pulse the components of the magnetization resulting from these two steps are

$$m_x = 0$$
$$m_y = 2m_0E_1\cos\,\theta\,\cos\,\theta'$$
$$m_z = 2m_0E_1\cos\,\theta\,\sin\,\theta'. \qquad [14]$$

The goal of the B subsequence is to obtain, from an initial $\pi/2$ pulse, the complementary sine modulation. By the end of this subsequence the magnetization components resulting from the two phase steps are

$$m_x = 0$$
$$m_y = 2m_0E_1\sin\,\theta\,\sin\,\theta'$$
$$m_z = 2m_0E_2\cos\,\theta\,\sin\,\theta'\cos\,\psi + 2m_0(1 - E_1)\cos\,\theta. \qquad [15]$$

Thus, summing up contributions of both subsequences and normalizing the result to one acquisition, we obtain for the signal amplitude

$$S(\delta, \Delta) = M_0\,\frac{E_1}{2}\,\overline{\cos\,\varphi}. \qquad [16]$$

This result is identical to that of Eq. [6] but, in the present context, it has been derived without any assumption.

Other phase cyclings can be considered. As an example, Table 1 shows a phase cycling more sophisticated that can be used to eliminate all residual magnetization resulting from imperfect $\pi/2$ and π pulses.

Figure 4 compares signals of octanol obtained from the basic and improved sequences, respectively. This figure demonstrates that oscillations can be totally removed and thus clearly illustrates the efficiency of this improved sequence even under extreme experimental conditions such as very small δ values, large Δ/T_1 ratio, small object dimensions, and low diffusion coefficient. Moreover, its robustness and its reliability have been tested extensively for one year by successful applications to the study of various system such as zeolites and porous systems (*13*), polymers, surfactants, and membranes.

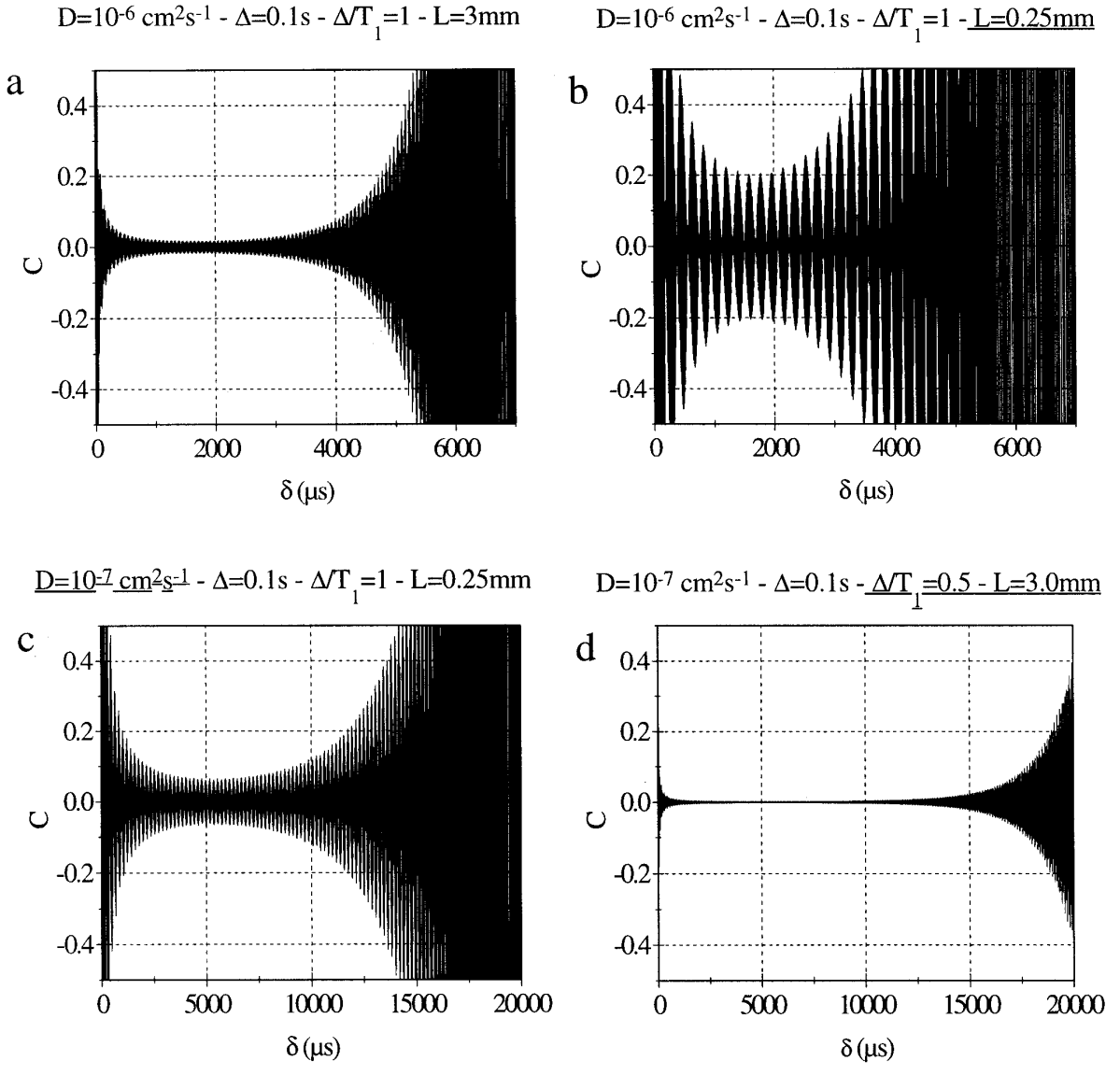

FIG. 5. Variation of the quantity C (Eq. [11]) versus δ for various sets of parameters D, L, Δ, and Δ/T_1. g_1 = 50 G cm^{-1}; apparent π pulse duration = 4.5 μs.

ADDITIONAL PROBLEMS

Short T_{12}

In many materials, especially those with slow molecular motions, the relaxation during the gradient pulses is not negligible and contributes to the signal attenuation (Eq. [1]). Not accounting for this relaxation phenomenon may lead to overestimate the self-diffusion coefficients and possibly to misinterpret the diffusion process, assigning for example the apparent biexponential behavior of Fig. 7 to two types of diffusion. There are two solutions to overcome this problem. The first one merely consists in removing the T_{12} relaxation contribution from raw data. T_{12} can be determined either by a basic rotary echo experiment (*11, 14*), δ_x–δ_{-x}–π/2-acq., in which δ is varied or simply from the relation $1/T_{12} = (1/T_1 + 1/T_2)/2$ (*15*), T_1 and T_2 being deduced from classical experiments. Alternatively, the determination of T_{12} from independent experiments is not compulsory since a complete fit according to Eq. [1] yields in principle appropriate values for both T_{12} and D, although the resulting accuracy is likely to be altered. The second solution is to keep constant the T_{12} contribution by choosing an adequate setting of δ and varying only the g_1 amplitude. This can easily be achieved by changing the input signal intensity of the linear amplifier which supplies the coil generating the RF gradient. From the consistent results shown in Fig. 8, this method seems to be a good alternative.

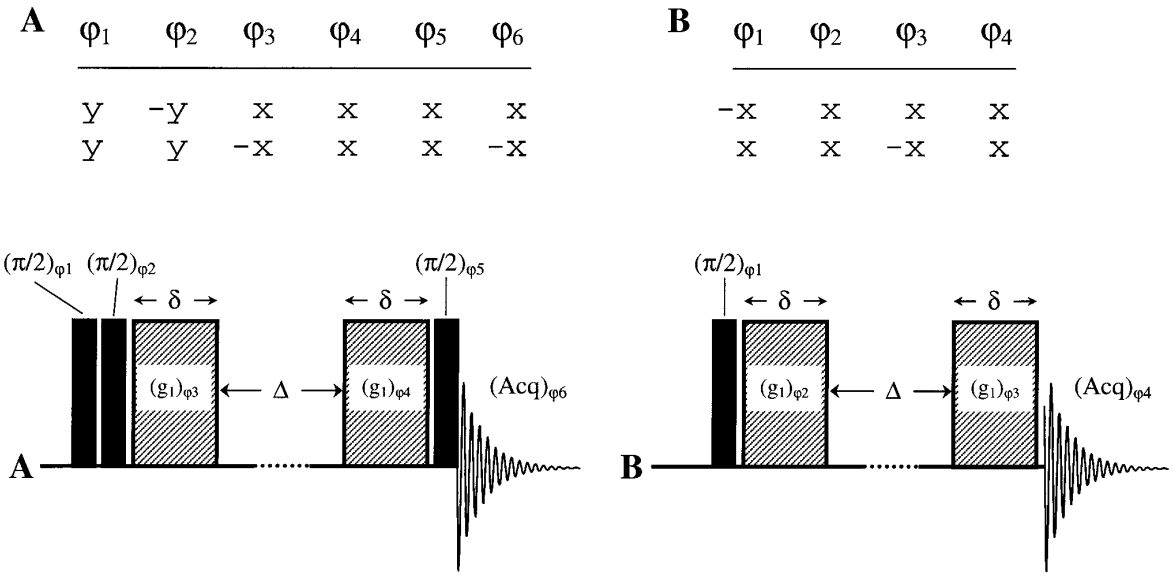

FIG. 6. Improved pulse sequence for removing the modulation observed in Figs. 3 and 4 while retaining the signal attenuation due to diffusion. The various symbols have the same meaning as in Fig. 1.

RF Power Amplifier Deficiency

In this technique by RF field gradient, the quality of measurements as well as the range of measurable diffusion coefficients is closely related to the performance of the RF power amplifier. Besides the output power, both key features are obviously the maximum pulse width, usually between 10 and 20 ms, and the maximum pulse duty cycle which is about 10%. In principle when the permitted values for both the pulse width and the duty cycle are not exceeded, the two gradient pulses in the diffusion sequence should be equivalent in terms of power. Actually, this is not always the case. An excellent test to check the equivalence of both gradient pulses consists in applying the rotary echo se-

TABLE 1

Another Possible Phase Cycling for the Sequence of Fig. 6 Designed for Improving the Elimination of Unwanted Magnetization

Sub-sequence A

φ_1	φ_2	φ_3	φ_4	φ_5	φ_6
y	−y	x	x	x	x
y	−y	x	−x	x	x
y	−y	−x	x	x	x
y	−y	−x	−x	x	x
y	y	x	x	x	−x
y	y	x	−x	x	−x
y	y	−x	x	x	−x
y	y	−x	−x	x	−x

Sub-sequence B

φ_1	φ_2	φ_3	φ_4
x	x	x	−x
x	x	−x	x
−x	x	x	x
−x	x	−x	−x
x	x	x	−x
x	x	−x	x
−x	x	x	x
−x	x	−x	−x

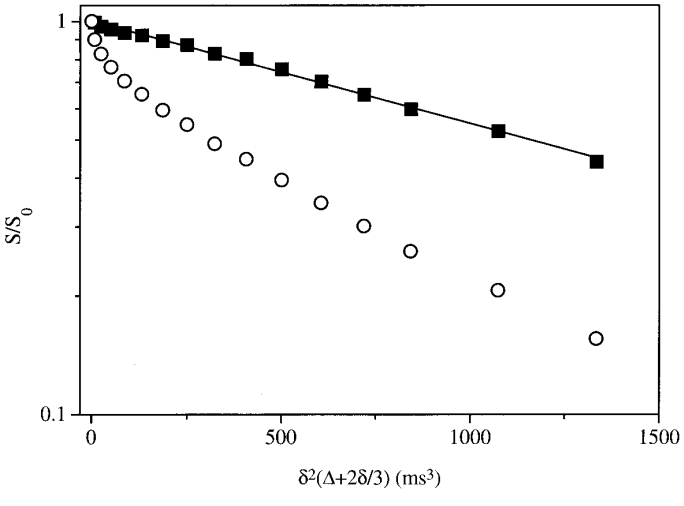

FIG. 7. Semi-logarithmic plot of the signal attenuation of water in hydrated heteropolyacids of the type $H_3PW_{12}O_{40}$ (*13*) versus $\delta^2(\Delta + 2\delta/3)$ using the sequence in Fig. 6. ○, raw data; ■, T_{12} corrected data. $g_1 = 51$ G cm^{-1}; $T_1 = 20.6$ ms; $T_2 = 8.2$ ms; $T_{12} = 11.7$ ms; $\Delta = 50$ ms; $T = 26°C$. *From these* T_{12} corrected data, a fit using Eq. [2] yields $D = 3.3\ 10^{-7}$ cm^2 s^{-1}.

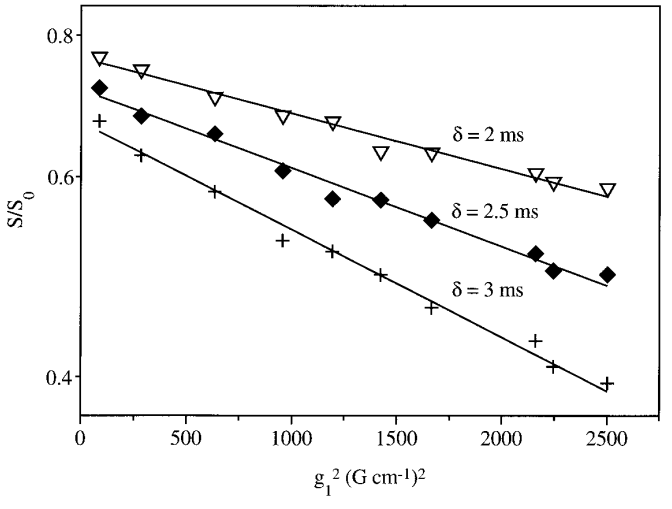

FIG. 8. Semi-logarithmic plot of the signal attenuation of water in hydrated heteropolyacids of the type $H_3PW_{12}O_{40}$ versus g_1^2 for various gradient pulse duration δ. g_1 ranges from 6 to 50 G cm^{-1}. T_1 = 20.6 ms; T_2 = 8.2 ms; T_{12} = 11.7 ms; Δ = 50 ms; T = 26°C. A Bruker Blax-300 wideband RF amplifier was used.

quence to a compound with a small diffusion coefficient and a sufficiently long T_{12}. The amplifier response pseudo-curve is then obtained by varying the gradient pulse duration. Figure 9 shows such curves obtained with a Bruker Blax-300 wideband RF amplifier at 90 MHz. Similar results have also been obtained at 300 and 400 MHz with other amplifiers of the same design. As shown in Fig. 9, when the interval Δ between the two gradient pulses becomes smaller than about 300 ms (at least in the examined δ range) the curves are severely distorted even for the δ/Δ ratios below the maximum duty cycle leading eventually to strong unwanted oscillations. Consequently, the diffusion measurements performed under these conditions are dramatically affected and even in certain cases are impracticable. Indeed, the smaller is the diffusion coefficient and/or the smaller is Δ (dictated by short longitudinal relaxation times) the more predominant is the signal attenuation arising from the amplifier deficiency with respect to attenuation due to diffusion. This effect is clearly seen in Fig. 10 where the damping coefficient $\gamma^2 g_1^2 D_{app}\Delta$ (D_{app} standing for apparent diffusion coefficient) is plotted as a function of Δ. A way of circumventing this problem is to replace the second gradient pulse in the diffusion sequence with a train of pulses, one data point being acquired between two consecutive pulses in such a way that the whole rotary echo is sampled, allowing for the measurement of the echo maximum. Dupeyre *et al.* (*11*) have already suggested this method to overcome the amplifier instabilities. However, in our case, we are not really dealing with an instability problem, the amplifier response being quite reproducible, all other things being equal. Obviously a better solution lies rather in the improvement of the amplifier response curves. Different tests have revealed that the problem originates essentially from an impedance mismatch between the amplifier output and the probe even if the latter is perfectly tuned. This mismatch entails a reflected power level which, without being excessive, is sufficient to perturb the amplifier final stage transistors and to modify slightly the amplifier features. This deficiency, which is certainly more specific to wideband amplifiers, is more or less important depending on frequency, on output power, on probe tuning and also on leakage between the gradient coil and the receiver coil. These considerations led us to design a system for adjusting easily the amplifier output impedance and thus reducing this mismatch problem. This system, described in detail elsewhere, greatly improves the amplifier response curves, as illustrated in Fig. 9 (an excellent agreement with the theoretical curve exists as long as the conditions on duty cycle are respected), and thereby the accuracy of diffusion measurements especially in systems with small diffusion coefficients and short relaxation times (Fig. 10). Notice that, in Fig. 10, the linear least-squares fit of data obtained by using this system goes through zero confirming the accuracy of measurements performed for small Δ values.

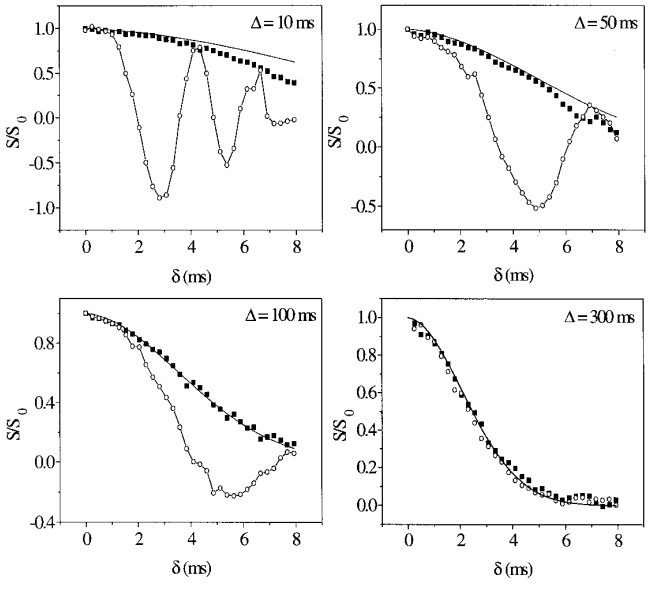

FIG. 9. The signal amplitude vs the incremented gradient pulse width δ, as obtained by the simple rotary echo sequence $[\delta_x\text{–}\Delta\text{–}\delta_{-x}\text{–}\pi/2\text{–acq.}]_n$ (the NMR signal being on resonance and acq. corresponding to only one data point), using a Bruker Blax-300 wideband RF amplifier with (■) and without (○) the circuit devised for correcting the amplifier output impedance. The solid line is the theoretical curve arising from Eq. [1]. The sample is neat $C_6F_{13}C_2H_4SC_2H_4(OC_2H_4)_2OH$, a surfactant whose diffusion coefficient is weak (D = 2.05 10^{-7} cm^2 s^{-1}). The other parameters are T_1 = 201 ms; T_{12} = 126 ms; g_1 = 50 G cm^{-1}; L = 3 mm; T = 26°C. Note that (i) as the signal is "on resonance" and as only one point is acquired, the two phase steps of Fig. 1 become useless; (ii) the values of D, Δ, Δ/T_1, L, and g_1 are such that the data inaccuracy is as low as 2% for the considered δ range (see Fig. 5d) and lead consequently to representative curves.

CONCLUSION

Diffusion measurements by RF gradient can suffer from three types of artifacts arising respectively from: (1) a non-complete magnetization defocusing during the gradient pulses, (2) very short relaxation times, (3) RF power amplifier deficiency. (i) A slight modification of the basic sequence, (ii) a procedure involving the increment of the gradient amplitude rather than the gradient pulse length, and (iii) a fine adjustment of the amplifier output impedance, proved to eliminate almost entirely these artifacts. As illustrated in Fig. 11, these remedies make the method especially robust and enable one to consider almost all types of diffusion processes, ranging from rapid diffusion in the gas phase ($D \approx 0.6$ cm^2 s^{-1}) to very slow diffusion in e.g., surfactant systems ($D \approx 8\ 10^{-9}$ cm^2 s^{-1}). Moreover, although RF gradients present performances comparable to B_0 gradients for small samples, it is not proven that such extreme measurements could be performed with the latter because of (i) the requirement of fast switching in the case of large diffusion coefficients and (ii) their sensitivity to background gradients in the case of slow diffusion in heterogeneous samples.

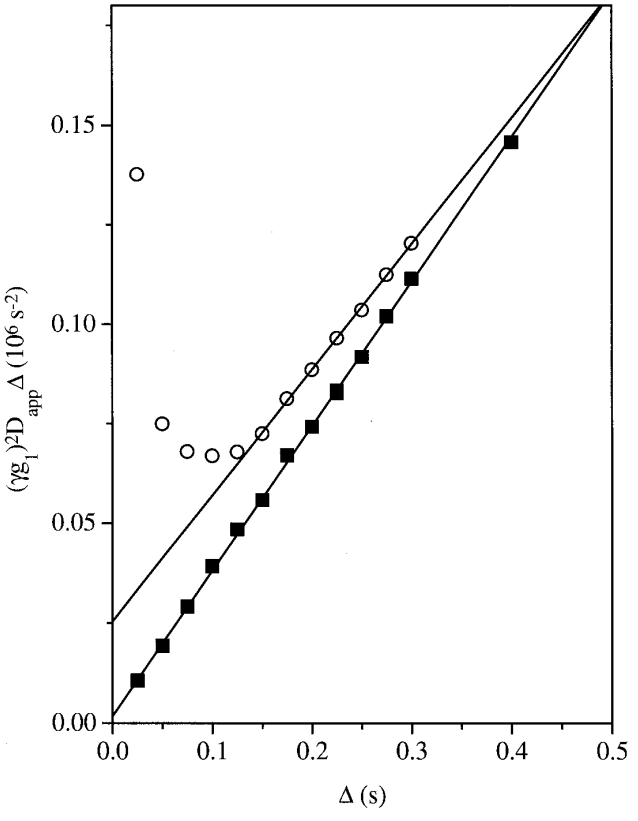

FIG. 10. Plot of the decay rates $(\gamma g_1)^2 D_{app} \Delta$ as a function of Δ, deduced from data analogous to those of Fig. 9, obtained however with the sequence of Fig. 6 with (■) and without (○) the circuit devised for correcting the amplifier output impedance while respecting duty cycle ($\Delta \geq 10\delta$). The decay rates result from a fit vs δ^2 according to Eq. [1]. Note that the straight line corresponding to the data represented by filled squares goes through the origin as theoretically expected.

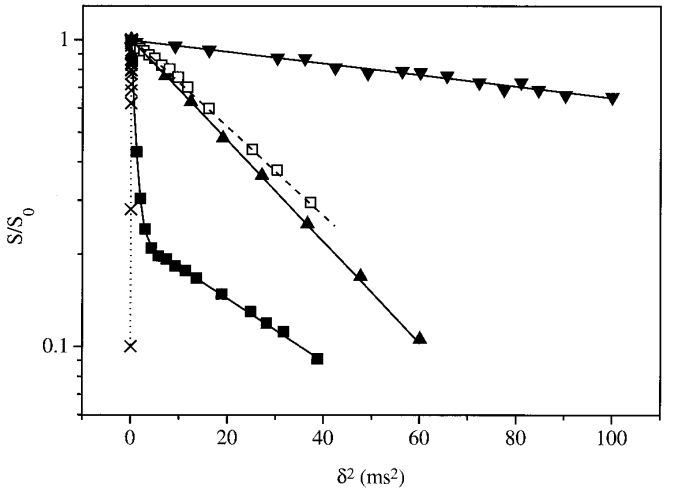

FIG. 11. Plots of the signal attenuation due to the molecular self-diffusion versus δ^2 using the sequence of Fig. 6 for various systems: (x) CH_4 200 mbars, $\Delta = 0.2$ ms, δ ranging from 10 to 50 μs, $T_1 = 10$ ms, $T_2 = 4.5$ ms; $T = 26$°C, $\mathbf{D = 0.62\ cm^2\ s^{-1}}$ (in agreement with the gas kinetic theory); (□) water in hydrated heteropolyacids of the type $H_3PW_{12}O_{40}$, $\Delta = 50$ ms, $T_1 = 20.6$ ms, $T_2 = 8.2$ ms, $T_{12} = 11.7$ ms, $T = 26$°C, $\mathbf{D = 3.3\ 10^{-7}\ cm^2\ s^{-1}}$; (■) $(CH_3)_4NCl$ (aqueous solution 0.5 *M*) inside and outside a Nafion membrane of 200-μm thickness, $\Delta = 100$ ms, $T_{1\ \text{inside}} \approx 1$ s, $T_{1\ \text{outside}} \approx 5$ s, $T = 13$°C, $\mathbf{D_{inside} = 6.7\ 10^{-8}\ cm^2\ s^{-1}}$, $\mathbf{D_{outside} = 5.7\ 10^{-6}\ cm^2\ s^{-1}}$ derived by treating the data according to a biexponential function; (▲) neat $C_6F_{13}C_2H_4SC_2H_4(OC_2H_4)_2OH$, $\Delta = 200$ ms, $T_1 = 201$ ms, $T_2 = 92$ ms, $T_{12} = 126$ ms, $T = 26$°C, $\mathbf{D = 2.05\ 10^{-7}\ cm^2\ s^{-1}}$ (consistent with the literature data concerning similar compounds); (▼) neat $C_6F_{13}C_2H_4SC_2H_4(OC_2H_4)_2OH$, $\Delta = 300$ ms, $T_1 = 101$ ms, $T_2 = 5$ ms, T_{12} 10.2 ms, $T = -20$°C, $\mathbf{D = 8.3\ 10^{-9}\ cm^2\ s^{-1}}$ (value confirmed by other measurements performed for various Δ and consistent with the activation energy). The diffusion coefficients result from a fit using Eq. [2] on T_{12} corrected data.

ACKNOWLEDGMENTS

We are grateful to Professor J. M. Dereppe (Louvain la Neuve), Professor P. Turq (Paris), and Dr. M. J. Stebe (Nancy) for supplying respectively the heteropolyacid samples, the membranes, and the surfactant used in this study and thus for inciting us to extend the range of applications of the technique.

REFERENCES

1. E. O. Stejskal and J. E. Tanner, Spin diffusion measurements; spin echoes in the presence of a time-dependent field gradient, *J. Chem. Phys.* **42,** 288 (1965).
2. P. T. Callaghan, "Principles of Nuclear Magnetic Resonance Microscopy," Oxford Univ. Press, Oxford (1993).
3. J. Zhong, R. P. Kennan, and J. C. Gore, Effects of susceptibility variations on NMR measurements of diffusion, *J. Magn. Reson.* **95,** 267 (1991).
4. X. Hong and W. T. Dixon, Measuring diffusion in inhomogeneous systems in imaging mode using antisymmetric sensitizing gradients, *J. Magn. Reson.* **99,** 561 (1992).
5. J. Lian, D. S. Williams, and J. J. Lowe, Magnetic resonance imaging

of diffusion in the presence of background gradients and imaging of background gradients, *J. Magn. Reson. A* **106,** 65 (1994).

6. D. van Dusschoten, P. Adrie de Jager, and H. van AS, Flexible PFG NMR desensitized for susceptibility artifacts, using the PFG multiple-spin-echo-sequence, *J. Magn. Reson. A* **112,** 237 (1995).
7. G. S. Karczmar, D. B. Twieg, T. J. Lawry, G. B. Matson, and M. W. Weiner, Detection of motion using B_1 gradients, *Magn. Reson. Med.* **7,** 111 (1988).
8. D. Canet, B. Diter, A. Belmajdoub, J. Brondeau, J. C. Boubel, and K. Elbayed, Self-diffusion measurements using a radiofrequency field gradient, *J. Magn. Reson.* **81,** 1 (1989).
9. R. Raulet, J. M. Escanyé, F. Humbert, and D. Canet, Quasi-immunity of B_1 gradient NMR microscopy to magnetic susceptibility, *J. Magn. Reson. A* **119,** 111 (1996).
10. F. Humbert, B. Diter, and D. Canet, NMR Microscopy by strong radiofrequency-field gradients with spatial resolution better than five micrometers, *J. Magn. Reson. A* **123,** 242 (1996).
11. R. Dupeyre, Ph. Devoulon, D. Bourgeois, and M. Décorps, Diffusion measurements using stimulated rotary echoes, *J. Magn. Reson.* **95,** 589 (1991).
12. D. Canet, Radiofrequency field gradient experiments, *Prog. NMR Spectrosc.* **30,** 101 (1997).
13. J. M. Dereppe, C. Moreau, and F. Humbert, NMR diffusion measurements in heterogeneous media using pulsed radio frequency field gradients, *Microporous Materials,* in press.
14. I. Solomon, Rotary spin echoes, *Phys. Rev. Lett.* **2,** 301 (1959).
15. H. C. Torrey, Transient nutations in nuclear magnetic resonance, *Phys. Rev.* **76,** 1059 (1949).